ISSN 1063-7745, Crystallography Reports, 2021, Vol. 66, No. 5, pp. 711–725. © Pleiades Publishing, Inc., 2021.
Russian Text © The Author(s), 2021, published in Kristallografiya, 2021, Vol. 66, No. 5, pp. 681–696.

REVIEWS

# The Integrative Approach to Study of the Structure and Functions of Cardiac Voltage-Dependent Ion Channels

**Y. G. Kacher[a], M. G. Karlova[a], G. S. Glukhov[a], H. Zhang[b], E. V. Zaklyazminskaya[c], G. Loussouarn[d], and O. S. Sokolova[a,b,*]**

[a] *Moscow State University, Faculty of Biology, Moscow, Russia*
[b] *MSU-BIT University, Shenzhen, China*
[c] *Petrovsky National Research Center of Surgery, Moscow, Russia*
[d] *L'unité de recherche de l'institut du thorax, Inserm, CNRS, Nantes, France*
**e-mail: sokolova@mail.bio.msu.ru*

Received September 3, 2020; revised September 15, 2020; accepted September 15, 2020

**Abstract**—Membrane proteins, including ion channels, became the focus of structural proteomics midway through the 20th century. Methods for studying ion channels are diverse and include structural (X-ray crystallography, cryoelectron microscopy, currently X-ray free electron lasers) and functional (e.g., patch clamp) approaches. This review highlights the evolution of approaches to study of the structure of cardiac ion channels, provides an overview of new techniques of structural biology concerning ion channels, including the use of lipo- and nanodiscs, and discusses the contribution of electrophysiological studies and molecular dynamics to obtain a complete picture of the structure and functioning of cardiac ion channels. Electrophysiological studies have become a powerful tool for deciphering the mechanisms of ion conductivity and selectivity, gating and regulation, as well as testing molecules of pharmacological interest. Obtaining the atomic structure of ion channels became possible by the active development of X-ray crystallography and cryoelectron microscopy, and, recently, with the use of XFEL.

**DOI:** 10.1134/S1063774521050072

## TABLE OF CONTENTS

Introduction

1. Cardiac ion channels and channelopathies: why do we need to know the structure of ion channels?

2. The path to a full-size ion channel structure

3. Structural and functional studies of ion channels

4. Electron microscopy for the study of ion channels

5. A revolution in structural biology—cryo-EM structures of ion channels at near-atomic resolution

6. New strategies for the purification of ion channels

6.1. Why is it so difficult to study the structure of membrane proteins?

6.2. Nanodiscs

6.3. Lipodiscs

7. Study of ion channel dynamics using X-ray free electron lasers

Conclusions

## INTRODUCTION

The 20th century was a blossoming time for structural biology—an enormous amount of structural data was obtained and a real potential for the reconstruction of all processes in living organisms was accumulated. Two decades of the 21st century are over and more than 160000 tertiary and quaternary protein structures have been deciphered; these include large molecular machines, ribosomes [1], membrane proteins [2, 3], cytoskeleton proteins [4], enzymes, etc. Optimists predict solving the structures of all known proteins and their functions in the upcoming 30 years. This means not only understanding the structure of individual macromolecules and their interactions with ligands, but also intermolecular interactions in protein complexes. Conformational changes that occur in a protein reflect its functional activity [5]. Obtaining comprehensive knowledge of the structure of a protein molecule makes it possible to correctly interpret its conformational changes during activation and inhibition, and to learn how to control these processes [6].

Following genomics, proteomics, transcriptomics, and metabolomics, "structural proteomics" emerged. Understanding biological mechanisms at the atomic level allowed to apply this information to medicine

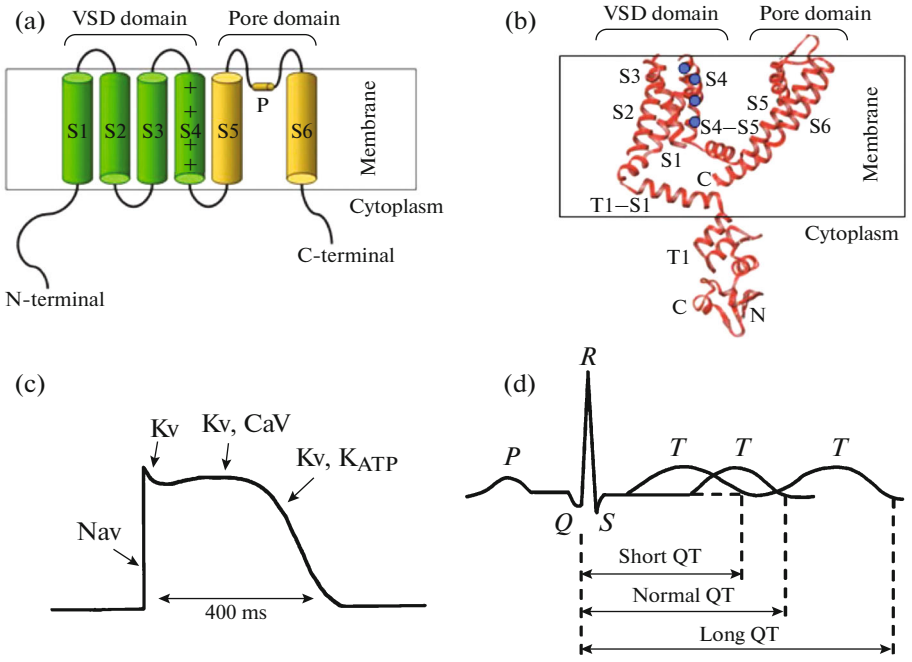


**Fig. 1.** Structure and functioning of the VD ion channels. (a) Schematic of one α-subunit of a Kv channel. Transmembrane segments S1–S6 and pore loop P are marked. Charged Arg within the S4 segment are indicated by plus signs. VSD—voltage-sensing domain. (b) Crystal structure of α-subunit of channel Kv1.2 (PDB ID 2A79). (c) Schematic of cardiac AP. The arrows indicate the ion channels responsible for the different phases of AP. (d) Normal intervals on ECG and altered intervals, characteristic for LQT and SQT syndromes.

and biotechnology. This is relevant for the study of membrane proteins, in particular ion channels and transporters, which take part in regulating the vital functions of every cell in the body, especially cardiomyocytes.

Ion channels are a large functional class of integral transmembrane proteins. Most ion channels possess a rotational symmetry formed by several identical subunits or homologous domains around the channel pore. Ion channels can be classified by their gating mechanism: voltage-gated, ligand-gated, light-gated, mechanosensitive, cyclic nucleotide-gated, and calcium-gated.

Voltage dependent (VD) ion channels are the most extensive group. Their role in excitable cells is to de- or repolarize membranes in response to changes in the potential. The structural unit of most of the VD channels that conduct $K^+$, $Ca^{2+}$, and $Na^+$ ions consists of four subunits or four domains, each formed by six helixes (Fig. 1b), crossing the lipid bilayer. Their function is determined by the coordinated operation of three structural units: the voltage sensor (helixes 1–4), pore, and channel gate (helixes 5 and 6, Figs. 1a, 1b).

Action potentials (AP) in the cells differ significantly from those found in other cell types. This happens due to the presence of heart-specific ion channels (mostly expressed in cardiomyocytes) and the specific kinetics of their work. Rapid Nav channels are responsible for the depolarization of the myocyte membrane, while the Cav ion channels are activated during the plateau phase. Kv channels play a crucial role in determining the phase of repolarization (Fig. 1c).

## 1. CARDIAC ION CHANNELS AND CHANNELOPATHIES: WHY DO WE NEED TO KNOW THE STRUCTURE OF ION CHANNELS?

The rhythmic contraction of the heart throughout a person's life course is provided by the synchronous generation and propagation of electrical impulses provided by the well-coordinated operation of several dozen ion channels. Voltage-dependent cation channels and accessory proteins encoded by the *KCNQ1*, *KCNH2*, *KCNE1*, *KCNE2*, *KCNJ2*, and *TRPM4* genes play an important role in the repolarization of cardiac cells and in the maintenance of the normal duration of cardiac AP.

The Kv7.x or KCNQ family includes five channel types (Kv7.1–Kv7.5). The Kv7.1 channel, encoded by the *KCNQ1* gene, is predominantly expressed in the cardiac tissue, as well as in the epithelial tissue and the smooth muscles. Kv7.2–Kv7.5 (*KCNQ2–5*) channels are mainly found in the nervous system [7]. In the cardiac muscle, Kv7.1 is expressed together with the auxiliary *KCNE1*, *KCNE2*, and *KCNE3* subunits to form a functionally active channel that provides a slow repolarization current [8], and, therefore, is responsible for

the duration of cardiac AP. To date, more than 300 mutations (mainly single nucleotide variations, SNV) are described affecting the activity of the Kv7.1 channel, altering the kinetics of activation and interaction with regulatory subunits, disrupting traffic to the cell membrane. Some alterations lead to the development of a prolonged QT interval (type 1 Long QT syndrome, LQTS) on the electrocardiogram (ECG) (Fig. 1d), may manifest by sudden cardiac death (SCD). In addition to this dominant form of LQTS, some of these mutations are associated with the recessive Jervell and Lange-Nielsen syndrome [9], a condition in which heart rhythm disturbances are accompanied by hearing impairment. On the other hand, gain-of-function mutations that cause an increase in current and lead to the shortening of the AP duration (Short QT syndrome, short QT, SQTS) and atrial fibrillation [10] have been also described for this channel.

The correct functioning of ion channels can be disrupted by mutations that affect the number of expressed protein subunits, the primary and secondary structures, and protein post-translational modifications. As a result of genetically determined changes, the total ion permeability through the channel may increase (activation or inactivation gates are open more frequently at a given potential) or decrease (gates are more frequently closed at a given potential). Notably, mutations that alter functional effects can lead to clinically opposite electrocardiographic phenomena, and, as a result, the corresponding arrhythmogenic syndromes. A well-studied example of such allelic series are syndromes that develop as a result of various mutations in the *KCNH2* gene. Loss-of-function mutations (for example, substitutions of N410D, A561T, G610S, A614V, N996I, etc.) lead to a decrease in the total outflow potassium current from the cell, which delays repolarization and leads to the QT prolongation [11]. This genetic form is the second most common subtype of hereditary LQTS (type 2 LQTS), a disease with a high risk of developing 'torsade de pointes' type ventricular tachycardia and sudden cardiac death [12]. Mutations in this gene account for 35% of all genetically confirmed cases of LQTS [13].

Gain-of-function *KCNH2* mutations lead to an increased outward flux of positively charged potassium ions, which results in the acceleration of repolarization and is manifested by abnormally short QT intervals on the ECG (Fig. 1d). The electrocardiographic and clinical manifestations of such mutations are more diverse, and include short QT syndrome (T618I replacement), Brugada syndrome (e.g., T152I, R164C, W927G, R1135H, etc.), familial atrial fibrillation (N588K variant) [14–16].

The functioning of the Kv11.1 channel (encoded by the *KCNH2* gene) can be altered not only by mutations, but also by interactions with a wide range of drugs. The blocking of the Kv11.1 channel with the development of secondary cardiac AP duration prolongation (and, as a consequence, prolongation of the QT interval) is a common, very dangerous side effect of a wide range of drugs. Terfenadine, a histamine H1-receptor antagonist, was the first drug withdrawn from the pharmacological market in 1998, due to the blockage of the Kv11.1 channel and the risk of ventricular arrhythmias; later at least a dozen similar drugs followed [17]. Currently, all new pharmaceutical substances are being tested for their ability to block cardiac ion channels, mainly Kv11.1. Understanding the structure and functioning of ion channels (Kv11.1, in particular) is very important for the rational design of new drugs. It was shown that some amino acids in the S6 domain (Tyr652, Phe656) and at the base of the pore helix (Thr623, Ser624, Val625) are especially susceptible to drugs [18]. Regardless of the direction in which the duration of cardiomyocyte repolarization is shifted, the main threat to carriers of mutations in the *KCNH2* gene is the increased risk of developing ventricular arrhythmias and sudden death.

Treatment efficacy of different hereditary cardiac channelopathies varies. Currently, both surgical (implantation of antiarrhythmic devices and left stellectomy) and conservative medication-based approaches are available. Beta-blockers have shown high, yet not absolute efficiency in LQTS treatment [19]. However, such drug therapy is insufficient for other channelopathies (such as: familial cardiac conduction disease (CCD), Brugada Syndrome (BrS), short QT syndrome (SQTS)). Therefore, a detailed study of structural and functional changes in normal and mutant ion channels is necessary for the development of new molecules capable of compensating for the genetic defect.

New generation sequencing has led to an exponential increase in the number of genetic tests performed. A natural result of the growth of conducted diagnostic tests has been the identification of a large number of new, uncharacterized rare variants, the clinical significance of which is difficult to interpret. A detailed understanding of the structure of ion channels, the comprehension of the functional significance of each amino acid residue will help develop predictive models that will reliably foreshadow the value of new unique variants.

## 2. THE PATH TO A FULL-SIZE ION CHANNEL STRUCTURE

By the end of the 20th century, many genes encoding eukaryotic ion channels, as well as their bacterial analogues, had successfully been cloned. However, the quaternary structure of most of the ion channels remained unknown for a long period of time, since they hardly 3D crystallize. Conclusions about the structure and functioning of the channels were made based on indirect data from mutation analysis, elec-

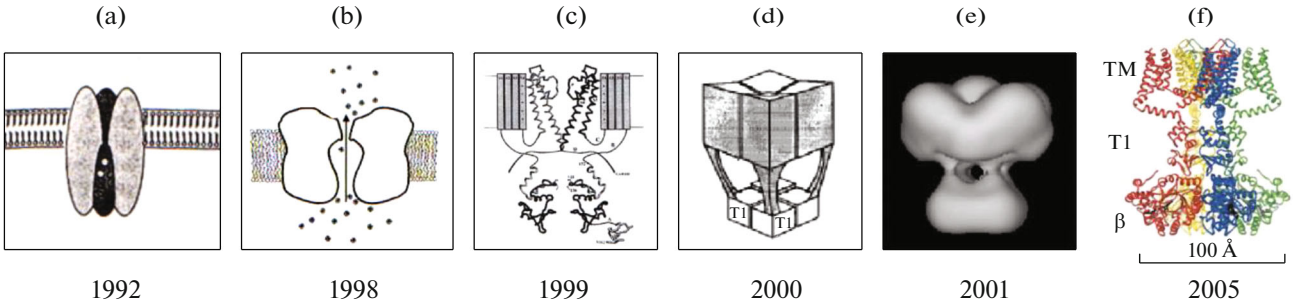


**Fig. 2.** The path towards the structure of the *Shaker* Kv channel. (a) Demonstration the tetrameric structure of the channel [20]; (b) data on the channel water pore obtained; (c) the structures of the pore domain (homologous channel KcsA [21]) and tetramerization domain were published [22]; (d) hypothesis of a "hanging gondola" [23]; (e) the first 3D EM structure of the *Shaker* channel [24] confirmed the abovementioned hypothesis; and (f) crystal structure of a chimeric full-size Kv1.1/1.2 channel in complex with β-subunit [25].

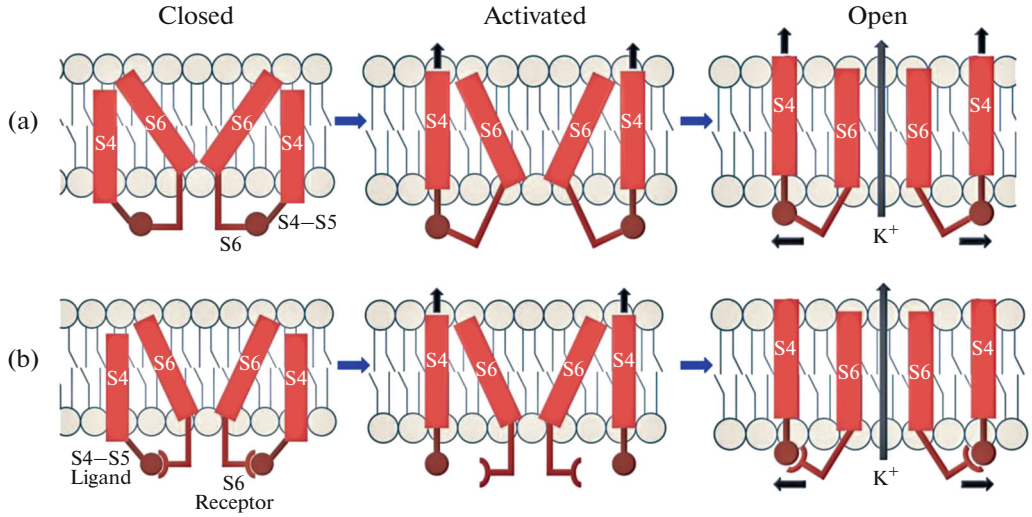


**Fig. 3.** Two models of the interactions between the voltage sensor and the pore subunits of the ion channel. (a) Mechanistic model is typical for *Shaker* family channels. (b) Ligand-receptor model is typical for EAG, ERG, KCNQ channels. The figure is adapted from [28].

trophysiology, and molecular dynamics (MD) (Fig. 2).

In the absence of direct structural data, comprehensive approaches were developed to solve the difficult task of determining the processes underlying the activation of Kv channels. This problem was partly solved by the early 1990s of the 20th century, when the first models of Kv channel activation were proposed (reviewed in [26]). According to cysteine scanning and electrophysiology data, it has been demonstrated that i) the Kv channel forms a tetrameter (Fig. 2); ii) in response to membrane depolarization, the S4 voltage sensor moves across the membrane [27], and iii) the S4 helix pulls the S4–S5 linker, which leads to the disturbance of the S4–S5/S6 interaction and, finally, to the opening of the channel pore [28] (Fig. 3a). However, some activation models were later found to be controversial [29]. Real structural data were needed to validate them.

The first crystal structure of the KcsA bacterial (*Streptomyces lividans*) ion channel with 3.2 Å resolution was obtained in the laboratory of the future Nobel Prize winner MacKinnon and published in 1998 [21]. This work has been cited more than 7000 times over the past 22 years. Since the pore structure is homologous in most cation channels [30], the KcsA structure has opened up priceless opportunities for structural biologists and biophysicists (Fig. 4).

The atomic structure of KcsA made it possible to use MD to model the conformations not only of this channel [31], but also of homologous eukaryotic channels [32, 33] (Fig. 4). To obtain well-diffracting crystals, the authors removed the intracellular C-terminal subunits of the KcsA channel. It was necessary to prove the functionality of the designed construct—the electrophysiology renaissance began.

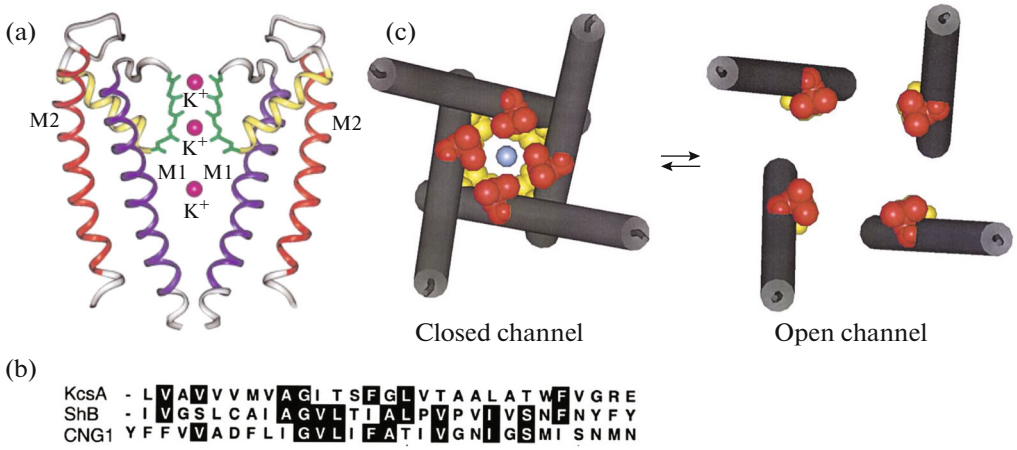


**Fig. 4.** (a) The crystal structure of the KcsA bacterial pH-dependent potassium channel allowed for molecular modelling of the homologous channel. Three potassium ions are located in the outer and inner selective filter positions (S1 and S3) and in the center of the water cavity. (b) Alignment of the sequences of the KcsA, *Shaker*, and the homologous CNG1 channel. (c) Modeling of the conformational changes upon opening and closing of the CNG1channel gate, based on MD data from [33].

## 3. STRUCTURAL AND FUNCTIONAL STUDIES OF ION CHANNELS

It is only possible to fundamentally understand how the structure of cation channels is altered by mutations through combining the expertise of structural studies and functional (electrophysiological) approaches. Characterization of ion channel activity, by use of electrophysiology, is the chief source of knowledge in both physiological and pathophysiological contexts, which, in turn, helps in the development of drugs.

In the 20th century, electrophysiology shed light on molecular mechanisms of conduction, selectivity, gating, and on the regulation of ion channels by accessory protein [34–39].

Regarding ion channel pathophysiology, electrophysiological tools, in particular the patch-clamp technique [40], were used in thousands of studies to confirm gene variants as being the cause of pathologies. A good example of this is the long QT syndrome, the monogenic inherited disease. It has long been at the center of the scientific community's attention, after the identification of several mutations, mainly in genes *KCNQ1*, *KCNH2*, and *SCN5A* [41, 42]. In many biophysical studies, the identified mutation was introduced in a plasmid coding for a channel, and patch-clamp experiments were undertaken to test if the mutation leads to a modification of the current.

Significant advances in high-throughput sequencing and genomic analysis have made it possible to study more complex forms of inherited diseases, such as BrS [43]. This syndrome is also a cardiac disorder characterized by ventricular fibrillation, which increases the risk of sudden cardiac death, as in the LQTS, but the pathophysiology is somewhat different: ECG monitoring easily distinguishes LQTS (characterized by prolonged QT interval) from BrS (ST segment elevation). In the LQTS, most of the cases have been linked to a specific mutation, mainly in *KCNQ1*, *KCNH2*, and *SCN5A* genes. In BrS, mutations in genes have only been identified in 20% of patients, in spite of the clear familial origin of the pathology. This is further complicated by the fact that often, when a gene mutation has been identified in a family (mainly *SCN5A*, which codes the voltage-gated sodium channel Nav1.5), some members of the family bear the mutation, but not the pathology (incomplete penetrance), and others present the pathology, but not the mutation (phenocopy) [44]. In such cases, electrophysiology tools such as patch-clamp are of great importance, even greater than for the LQTS, because they help understanding if the identified mutation led to channel dysfunction and whether it may, at least partially, participate to the pathogenesis.

In ion channel pathophysiology, electrophysiological tools are instrumental to delineate how disruption of a given molecular mechanism may lead to a pathology. For instance, patch-clamp studies showed that Kv7.1 and Kv11.1 channels require phospholipid Phosphatidylinositol 4,5-bisphosphate ($PI(4,5)P_2$), and that some long QT mutations alter the interaction of $PI(4,5)P_2$ with the channel and lead to a loss of channel function [45–47].

Lastly, examination of the intimate intramolecular interaction within voltage-gated channels allowed to design peptides mimicking these interactions and either inhibiting or activating the ion channel target group [48–51]. Such studies may, in the long term, lead to the development of new therapeutic agents.

In all these aforementioned aspects, the development of high throughput patch-clamp tools will be helpful. First, the major interest of functional validation of variants, mentioned above, combined with the

rapid increase of gene variants to be tested, more than 1000 in Kv11.1 (hERG) channel, motivates the development and use of such high throughput gene phenotyping. This tool also starts to be exploited for drug screening [52, 53].

It is also important to mention the limitations of patch-clamp, especially because it may lead to misinterpretations of protein functions. A typical example of this: the story of KCNE1, originally named MinK (minimal potassium channel), because it was wrongly thought to be an ion channel, based on the observation that its expression in *Xenopus* oocyte led to a slowly activating voltage-gated potassium current. Despite the very cautious interpretation of the results in the original article, further experiments confirmed this hypothesis [54, 55]. Yet, the current could only be observed when the mRNA was injected into *Xenopus* oocytes, but not in other models, which raised some doubts [56]. Only the cloning of the channel gene, *KCNQ1* (originally named $K_VLQT1$), the demonstration of its presence in *Xenopus* oocytes and of it generating a slowly activating voltage-gated current only in presence of KCNE1 confirmed that *KCNE1* was not coding the pore-forming subunit [38, 39], but an auxiliary subunit of the KCNQ1 channel.

## 4. ELECTRON MICROSCOPY FOR THE STUDY OF ION CHANNELS

In the 1990s, electron microscopy started being used to study the structure of ion channels. The channels were isolated from cell membranes using detergents (DDM, CHAPS, digitonin, and others), applied to carbon-coated grids and contrasted with heavy metal salts [24, 57–60], or studied by cryoelectron microscopy (cryo-EM) [61, 62].

The advantage of cryo-EM is that protein molecules are in a water environment, so their shape and conformation are preserved. Particles in ice have no preferential orientation compared to particles on the carbon layer. At the same time, the signal-to-noise ratio in cryo-EM is generally low, because of the low contrast of the protein molecules. In order to increase contrast, data from a very large number of projections are combined. The reconstruction of macromolecules from cryo-EM data has been ongoing for more than four decades, but in its early stages it only allowed for three-dimensional structures at a moderate resolution of 15–18 Å, and only for large ion channels, such as the ryanodine receptor (RyR) [63, 64].

Radiation damage is a significant barrier in obtaining high-resolution images [65]. To reduce radiation damage, special "low-dose" systems are used during image area selection, alignment and beam focusing to block the beam until the last step, image acquisition. Small exposures result in loss of resolution, noisy images, and, as a direct consequence, lack of high-resolution data. This, in turn, complicates the subsequent image processing to determine the three-dimensional structure of an object. Determining the Euler angles for globular molecules is particularly sensitive to noise in raw images and to errors in alignment and classification procedures. The small size of Kv channel molecules (10–15 nm in diameter) led to the loss of image contrast in the microscope and a low resolution of reconstruction.

For very short exposures, the ability of the detector to perceive every electron becomes critical. Such devices were designed in the 21st century which allow direct detection of electrons (direct detector of electrons, DDD) and obtaining 16 to 400 single frames per second exposure. Due to a special image processing procedure, motion correction, the images from all frames can be aligned with each other and summarized to increase the signal-to-noise ratio. This compensates for the movement of the particles in the ice [66].

## 5. A REVOLUTION IN STRUCTURAL BIOLOGY–CRYO-EM STRUCTURES OF ION CHANNELS AT NEAR-ATOMIC RESOLUTION

Within 15 years after the publication of the first structure of the ion channel, researchers have been able to decipher the atomic structure of a number of prokaryotic [21, 67, 68], archean [69], and eukaryotic ion channels using X-ray crystallography [70–72].

The revolution in the structural biology began with the publication of the first near-atomic structure of the TRP ion channel in 2013 [73], de novo obtained using cryo-EM, which, in particular, is associated with the beginning of the serial production of DDE. The development of new image analysis software [74] has tremendously accelerated the collection and analysis of hundreds of thousands of images of individual channel particles. In 2015, the cryo-EM was declared the method of the year by Nature magazine, and, two years later, in 2017, three founding scientists of this method—R. Henderson, J. Dubochet, and J. Frank—were awarded a Nobel Prize in Chemistry for developing the method. And that was just the beginning. Over the next 4 years, a technical breakthrough allowed many previously unknown structures of ion channels to be deciphered, including the cardiac channels KCNQ1 and KCNH2 [75, 76].

The first high-resolution cryo-EM studies of the EAG family channel revealed that the activation model, based on data on the structure of *Shaker* family channels [26, 77], was not suitable for describing the activation of the channels encoded by the *KCNH* genes [3, 49, 75, 78].

The structure of the membrane domain of *Shaker* family channels has a characteristic feature, which became clear after deciphering the first crystal structure of the chimeric channel Kv1.1/Kv1.2 [71]: its VSD

interacts not with its own pore domain, but with a domain belonging to a neighboring subunit (Figs. 5a, 5c).

Such architecture was called "domain swapped." This arrangement of transmembrane helixes was possible because of the long S4–S5 linker in *Shaker* family channels. The domain swapped architecture was not applicable to EAG channels because of their very short S4–S5 linkers; therefore, a S5 helix interacts with the VSD from the same subunit (Figs. 5b, 5d) [75].

A comparison of the open conformations of the chimeric Kv1.2/2.1 [71] and Kv11.1 [3] channels to the closed, due to interaction with calmodulin (CaM), Kv10.1 channel [75], led researchers to a new hypothesis on the functioning of EAG family channels (Fig. 6). The difference from the previous model is that the S4–S5 linker is given a smaller role, and the main change in the conformation of S6 helix occurs due to the lateral displacement of the S4 and S5 segments. The hinge that provides the conformation change of S6 is formed by two Gly: G648 in Kv11.1 and G460 in Kv10.1 [3].

In parallel, it has been suggested that the activation of EAG family channels takes place via a so-called "ligand-receptor" mechanism (Fig. 3b). In this case, the S4–S5 linker acts as an internal ligand that binds the lower part of the S6 helix and locks the channel in a closed state when the S4 VSD helixes are in a "down" state with negative potential. When the S4 helixes transit to the "up" state, the S4–S5 linker leaves its binding pocket on the S6 and the channel is opened. This molecular mechanism is in good agreement with the results of electrophysiological experiments obtained, in particular, on hERG channels [49, 79].

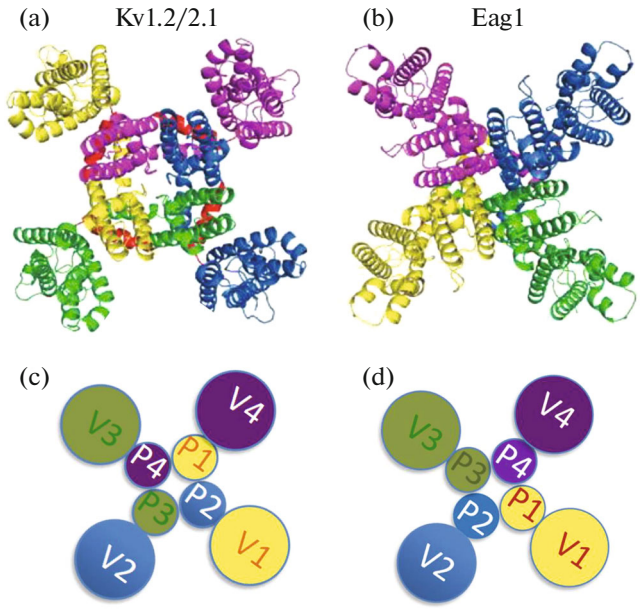


**Fig. 5.** Transmembrane domain interactions in Kv channels according to X-ray crystallography and cryo-EM. (a) Kv1.1/1.2 channel [25]; (b) Kv10.1 channel [75]. At the bottom, a schematic representation of the interaction between (c) pore domains and (d) VSD.

## 6. NEW STRATEGIES FOR THE PURIFICATION OF ION CHANNELS

### *6.1. Why Is It So Difficult to Study the Structure of Membrane Proteins?*

Structural studies require the production of the target protein in large quantities and with a high degree of purity. Nowadays, many different approaches to the production and purification of proteins have been developed. However, for membrane proteins, it is the sample preparation that is the bottleneck in determining their structure; in particular, the extraction of the target protein from cell membranes. A detergent that improperly mimics the hydrophobic environment of the protein of interest can also significantly alter its structure.

Under such conditions, 30 years ago, electron crystallography could only achieve the subnanometer resolution: the structures of bacteriorhodopsin in the purple membrane [80] and the acetylcholine receptor in the electric organ of the *Torpedo marmorata* [81] were obtained using this method. Later, it became possible to simulate natural two-dimensional crystals, using purified channel molecules and, by dialysis, removing the detergent from the mixture, replacing it with lipids. But this approach turned out to be quite difficult to reproduce and is still used in only a few laboratories in the world.

To obtain reconstructions of channel proteins in the membrane environment, other special approaches have also been developed, such as, for example, spherical reconstruction [82]. After insertion into a small spherical lipid vesicle, the membrane protein acquired a strictly defined orientation relative to the membrane, and its position on the projected image of the vesicle directly established two of the three determined Euler angles. The analysis of images of liposomes in ice showed that their density is well described by a simple model of electron scattering on a membrane. Computer simulations have shown that this method can theoretically improve the reconstruction of membrane proteins. We applied it to study the clustering of gramicidin in liposomes [83]; however, the method did not allow us to achieve high resolution.

The importance of lipids of the nearest environment has been shown for many proteins: for example, the interaction of $PI(4,5)P_2$ with Kv7 [45] and the interaction of KscA with anionic lipids [84]. The removal of these lipids upon solubilization with detergents can lead not only to functional impairments, but also to structural rearrangements. In this regard, both the search for new detergents and the development of fundamentally new approaches to the solubilization of membrane proteins are constantly being carried out. Relatively recently, two similar approaches, but based

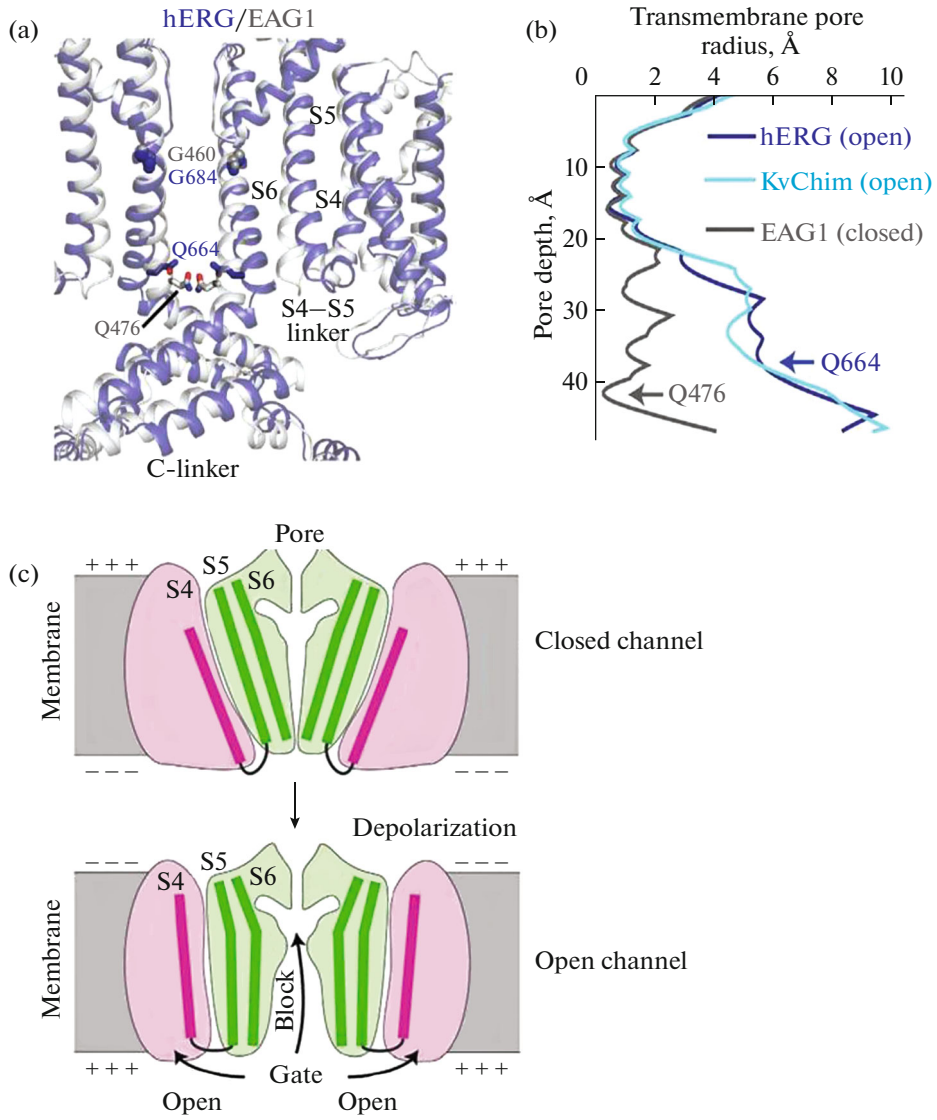


**Fig. 6.** Comparison of closed and open Kv channel structures. (a) Differences in the positions of the transmembrane part and the part adjacent to the pore in overlaid open Kv11.1 channel (dark grey) and closed Kv10.1 channel (light grey). (b) Comparison of pore profiles for open (hERG and Kv1.2/2.1) and closed (EAG1) channels. (c) Model of EAG family channel activation. Adapted from [3].

on different compounds, have been developed—the use of nanodiscs and lipodiscs in structural studies of membrane proteins.

### *6.2. Nanodiscs*

Nanodiscs represent an alternative and more efficient approach to the isolation of membrane proteins. These are simulators of the membrane environment (membrane mimetics) that can be used to maintain membrane proteins in a soluble form for further structural studies. As the name suggests, nanodiscs are disk-shaped nanoscale phospholipid bilayers surrounded by molecules of the amphipathic α-helical protein MSP, which acts as a belt that limits the size of the disk (Figs. 7a, 7c).

The method was originally based on the use of human apolipoprotein ApoA1. High density lipoproteins are composed of lipids and cholesterol, and the major apolipoprotein ApoA1 can take on various structural forms. It is synthesized in the liver, then, from a lipid-free form, it gradually takes the form of a ball of lipids, cholesterol, and cholesterol esters, passing through a temporary discoid stage. These discs became the prototype of water-soluble nanoparticles [87].

The incorporation of the membrane protein into the nanodiscs occurs spontaneously, since it interacts with hydrophobic lipid parts. Nanodiscs can be used over a wide concentration range at room and physiological temperatures and stored for several months at

4°C with minimal aggregation. Under the right conditions, monodisperse samples with a controlled size can be achieved. Currently, there are many modified variants of the MSP protein [88], including commercially available ones.

The quantitative and qualitative composition of nanodisc phospholipids can be varied to simulate the biological characteristics of certain membranes. The most popular synthetic lipids used to assemble nanodiscs are 1-palmitoyl-2-oleoyl-sn-glycero-3-phosphocholine (POPC), 1,2-dimyristoyl-sn-glycero-3-phosphocholine (DMPC), 1,2-dipalmitoyl-sn-glycero-3-phosphocholine (DPPC), and mixtures with charged phospholipids, such as $PI(4,5)P_2$, phosphatidylserine (PS), phosphatidylethanolamine (PE).

The publication of many structures of ion channels isolated in nanodiscs over the past five years clearly indicate the success of this method (Table 1). New variants of nanodiscs have emerged, which are adapted, among other things, for large proteins and complexes [89, 90], since the size of the nanodisc can be of decisive importance for maintaining the native oligomeric state of the protein incorporated into the nanodiscs. Moreover, for many types of nanodiscs, optimized protocols have already been published [91] and the optimal molar ratios of the lipid mixture have been selected.

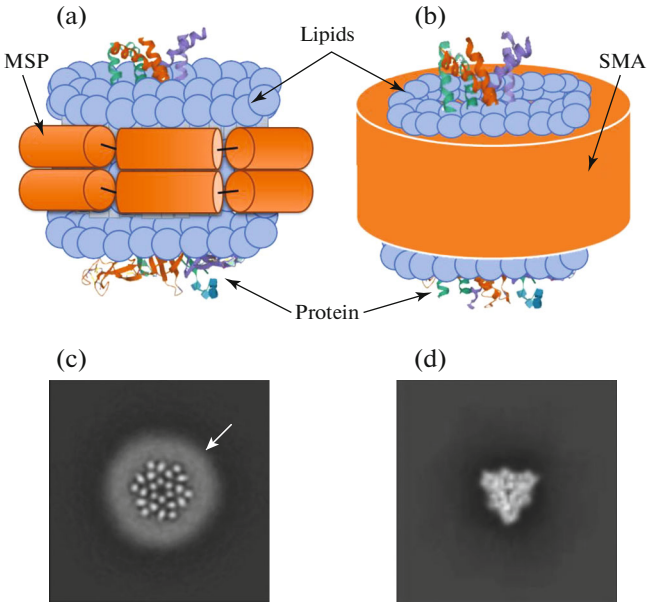


**Fig. 7.** Comparison of nanodisc and lipodisc complexes. Schematic representation of the nanodisc (a) and lipodisc (b) with an incorporated membrane protein. At the bottom, the cryo-EM class-sum averages of the channels, embedded in the nano- and lipodiscs: (c) dORAI channel in the MSP [85]. The arrow indicates the additional density corresponding to the nanodisc; (d) ASIC channel in SMA [86]. Note that the SMA does not form any extra-density around the membrane part of the channel, unlike the nanodisc.

### *6.3. Lipodiscs*

One of the recent approaches for isolating proteins in a natural lipid environment is the use of a styrene and maleic acid copolymer (SMA). An important feature of this polymer is the ability to switch between linear and helical conformations, depending on the pH and ionic strength of the solution. Alternating hydrophobic (styrene) and hydrophilic (maleic acid residues) fragments of SMA make it amphipathic, and, therefore, capable of incorporation into biological membranes. When embedded into the membrane, the polymer destroys it with formation of round fragments of 10–40 nm in diameter, surrounded by a polymer [106] (Fig. 7d). These fragments are called SMALP–Styrene Maleic Acid-lipid particles. The term "Lipodisq®" was introduced by Malvern Cosmeceutics Ltd. for proprietary polymer/lipid mixtures developed as vehicles for hydrophobic pharmacological substances. Currently, "lipodisc" or "native nanodisc" terms are mainly applied to disc-shaped membrane structures formed by polymers, as opposed to the term "nanodisc", which refers to structures formed by apolipoprotein derivatives (see above).

The effects of polymer composition (the ratio of styrene and maleic acid moieties), the pH of the medium, and the ionic strength of the solution on the solubilization efficiency of the model membrane are studied in detail in [107]. The polymer remains soluble in the pH range of 7–9, and it begins to aggregate with a lower pH. However, a polymer with a ratio of styrene and maleic acid residues of 1.4 : 1 can tolerate a pH decrease to 4. The high ionic strength of the solution reduces the solubility of the polymer, but increases the efficiency of membranes solubilization. Interestingly, the diameter of the resulting lipodiscs depends more on the lipid composition of the membrane, than on the characteristics of the polymer [108]. The length of the polymer molecules at a given ratio of styrene and maleic acid residues does not affect as much size of the particles, as their stability [109]. The size of the lipodiscs is affected by the mass ratio of lipid and polymer, as shown on the model system of the liposomes formed by a 9 : 1 mixture of POPC/POPG. After reaching a critical concentration of polymer required for the complete destruction of the vesicles, a further increase of polymer concentration leads to a decrease in the size of the lipodiscs [110].

The influence of the bilayer lipid composition on the kinetics of SMALP formation has been studied [111, 112]. It was shown that the length of the acyl chain of lipids has a slight effect on the size of lipodiscs, but determines the kinetics of SMALP formation. Bilayer packaging features are crucial for this process: the phase, membrane thickness, lateral pressure, charge density, temperature, and ionic strength of the solution. Thinner membranes with low lateral

**Table 1.** Ion channels whose structures are obtained in nanodiscs*

| Ion channel | Year | MSP type | Lipids | Structural method | Resolution | Ref. |
|---|---|---|---|---|---|---|
| KCC4 | 2020 | MSP1D1 | DOPE, POPC, POPS | Cryo-EM | 3.65 Å | [92] |
| VSD4-NavAb | 2020 | MSP1E3 | DMPC | EM | — | [93] |
| KCNQ1 and KCNE3 | 2020 | MSP2N2 | Soybean polar lipids | Cryo-EM | 3.1 Å | [94] |
| V/A-type ATPase | 2019 | MSP1E3D1 | POPC and *T. thermophilus* polar lipids | Cryo-EM | 3.5 Å | [95] |
| TMEM16F | 2019 | MSP2N2 | Soybean polar lipids, POPC, POPE, POPS | Cryo-EM | ~4 Å | [96] |
| AdeB | 2019 | MSP 1E3D1 | *E. coli* lipid extract | Cryo-EM | 2.98 Å | [97] |
| LRRC8A | 2019 | MSP1E3D1 | POPC | Cryo-EM | 4.18 Å | [98] |
| $H^+$-ATPase | 2019 | MSP1E3D1 | Yeast vacuolar lipids | EM | — | [99] |
| Orai | 2019 | MSP1E3D1 | POPC, POPG, POPE | Cryo-EM | 5.7 Å | [85] |
| TRPM4 | 2018 | MSP2N2 | Soybean polar lipids | Cryo-EM | ~3 Å | [100] |
| OSCA1.2 | 2018 | MSP2N2 | Soybean polar lipids | Cryo-EM | 3.1 Å | [88] |
| TPC1 | 2018 | MSP E3D1 and saposine A | Soybean polar lipids | Cryo-EM | 3.7 Å | [101] |
| Kv1.2–2.1 | 2018 | MSP1E3D1 | POPC, POPG, POPE | Cryo-EM | 3.3 Å | [102] |
| VDAC-1 | 2018 | DCND | POPC, POPG with cholesterol | EM | — | [90] |
| Kv7.1 | 2017 | MSP2N2 | No exogenic lipids | EM | 25 nm | [103] |
| TcdA1 | 2016 | MSP1D1 | POPC | Cryo-EM | 3.46 Å | [104] |
| TRPV1 | 2016 | MSP2N2 & MSP1E3 | Soybean polar lipids | Cryo-EM | No ligand–3.2 Å, with agonist–2.9 Å, with antagonist–3.4 Å | [105] |
| CorA | 2016 | MSP1D1 | POPC, POPG | Cryo-EM | 3.8 Å | [102] |

*Abbreviations: 1,2-dimyristoyl-sn-glycero-3-phospho-rac-(1-glycerol) (DMPG), 1,2-dioleoyl-sn-glycero-3-phospho-rac-(1-glycerol) (POPG), 1-palmitoyl-2-oleoyl-sn-glycero-3-phosphoethanolamine (POPE), 1-palmitoyl-2-oleoyl-sn-glycero-3-phospho-L-serine (POPS), 1,2-dioleoyl-sn-glycero-3-phosphoethanolamine (DOPE).

pressure, low surface charge density, and high NaCl concentrations dissolve faster and with a higher SMALP yield. It was shown that the polymer has no affinity for any specific lipids and the ratio of lipids in SMALP remains the same as it was in the native membrane. The thermodynamics of the SMALP formation were investigated on model membranes in [113]. The effect of the lipid composition on SMALPs formation is reflected in the kinetics of eukaryotic cell solubilization: according to fluorescence microscopy, intracellular membranes in the presence of SMA are destroyed faster and more efficiently than the plasma membrane [114]. The slower destruction of the plasma membrane may occur partly due to the presence of a large number of integral proteins.

If the polymer is added to a protein-containing membrane, protein molecules become enclosed in the forming lipodiscs; that is, the protein is cut out of the membrane, while preserving a certain layer of lipids surrounding it. This was initially demonstrated for liposomes formed by DMPC and containing bacteriorhodopsin [115]. Later, ABC transporters were extracted from the membrane fractions of various cell types [116], complex IV was extracted from the mitochondria of yeast cells [117], human voltage-gated potassium channel Kv7.1 was extracted from unfractionated eukaryotic cells [118] using the SMA copolymer. Membrane proteins enclosed in lipodiscs appear quite stable and can be purified and analyzed by different biochemical methods.

A significant advantage of using SMA is the complete absence of detergent in the protein purification protocol. As a result, the SMA-solubilized proteins can be extracted together with their natural lipid environment and ligands. This approach allows to increase the stability and maintain the functional activity of purified proteins and protein complexes, as has been shown for the human adenosine receptor A2A [119], voltage-gated potassium channel KcsA [120], AcrB *E. coli* transporter [121], photoreaction center (RC) from the purple bacterium *Rhodobacter (Rba.) sphaeroides* [122]. Often, SMA increases the overall yield of the solubilized protein, and also allows for single-stage purification [116, 118].

Preserving annular lipids of proteins extracted with a SMA copolymer opens up wide opportunities for the analysis of their natural lipid environment and lipid-protein interactions [123–125]. Co-extraction of lipids with membrane proteins was used to determine the lipid composition of *Saccharomyces cerevisiae* membrane microdomains [126].

The advantages of the SMA copolymer for membrane protein solubilization make it a promising tool for structural studies. Table 2 contains structures of proteins stabilized in lipodiscs published within the 2018–2020 period. Despite the relatively small number of papers on the matter, studies of ion channels stabilized with SMA become more popular and start showing resolution of reconstructions at subnanometer range.

**Table 2.** Ion channels whose structures are obtained in SMA using cryo-EM

| Ion channel | Year | Resolution | Ref. |
|---|---|---|---|
| KimA (*Bacillus subtilis*) | 2020 | 3.7 Å | [120] |
| ASIC1 | 2020 | 2.8, 3.7 Å | [86] |
| AcrB (*Salmonella typhimurium*) | 2020 | 4.6 Å | [127] |
| AcrB (*E. coli*) | 2018 | 8.8 Å | [128] |
| AcrB (*E. coli*) | 2018 | 3.2 Å | [129] |
| Alternative complex III (ACIII) (*Flavobacterium johnsoniae*) | 2018 | 3.4 Å | [130] |

## 7. STUDY OF ION CHANNEL DYNAMICS USING X-RAY FREE ELECTRON LASERS

With the design of X-ray free-electron lasers (XFEL) and micro-focus stations on synchrotron radiation sources, serial crystallography became the most important method for the study of small membrane proteins [131]. A new approach to the acquisition of diffraction data allows structural information to be collected from nano- and micro-crystals at room temperature with minimal radiation impact, by means of ultrafast data collection in less time than the characteristic time of the radiation damage of the crystal. The combination of the enormous brightness of the flash (over 10 W/cm$^2$ (focused on an area of about 100 nm$^2$)) and the short duration (about 10 fs) leads to the unique fundamental possibilities of this tool in structural biology.

When trying to crystallize membrane proteins, they often tend to form very small micro- or nanocrystals. The diffraction quality of such crystals is usually worse than that of soluble protein crystals of a similar size. In such cases, a better resolution of the crystal structure can be achieved by increasing the power of the X-ray source, while the pulse length should be shorter than the characteristic time of crystal collapse, i.e., a few fs. Recently, the lipid cubic phase (LQP) was used for crystallization of membrane proteins [132]. This approach and the development of special injectors for viscous solutions made it possible to develop a method of serial femtosecond crystallography (Fig. 8a). It allows collecting diffraction data from multiple microcrystals embedded in the LQP, with only one diffraction pattern per crystal in one orientation to be saved at a time. A large amount of such raw data is combined into one set. This method was instrumental in obtaining structures of important ion channels like the GPCR-receptor [133] and bacteriorodopsin [134]. The isomerization of bacteriorodopsin retinal is one of the fastest known biological reactions, and recently the light-induced molecular movements inside retinal (Fig. 8b), have been revealed at atomic resolution using XFEL [134].

## CONCLUSIONS

We are witnesses to the rapid developments in the structural research of ion channels. Over the last

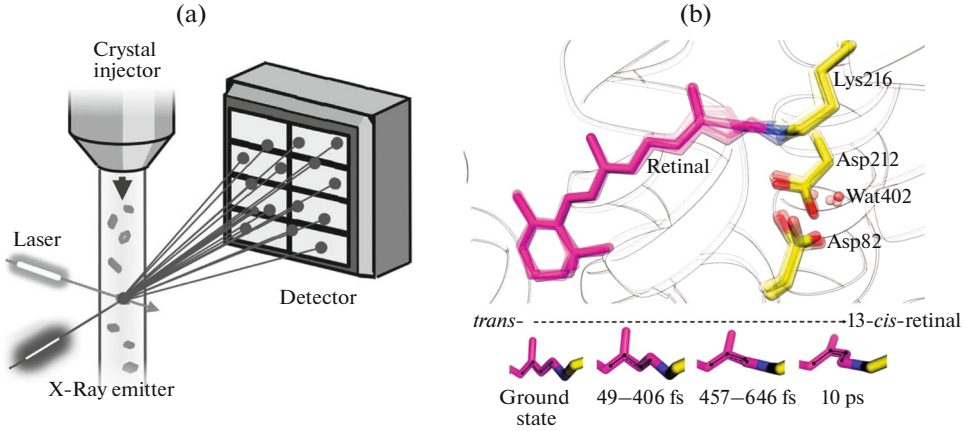


**Fig. 8.** Time-resolved serial femtosecond crystallography. (a) Installation setup and (b) light-induced time-resolved isomerization of bacteriorhodopsin retinal (from [134]).

5 years, more than 50 new structures of various ion channels have been obtained with the help of cryo-EM, which is several times more than those obtained with the help of X-ray crystallography in the recent 20 years. Cryo-EM revealed the structures of such ion channels, as the glutamate receptor [135] that previously could not be crystallized in full, due to their size and complex organization.

With the development of structural biology, electrophysiology has been used to validate new structures. As opposed to structural studies, functional research is easy to do in real time: opening and closing a channel takes milliseconds to seconds. Dynamics of cardiac channel activity are, thus, accessible, and the combination of mutagenesis and electrophysiology helps to sort out the functional relevance of structural data, which is very important for understanding the consequences of mutations in ion channels. As a recent and promising functional model, cardiomyocytes derived from induced pluripotent stem cells may be used, that express many proteins that are also present in mature cardiomyocytes, allowing data to be obtained simultaneously for tens of cardiac ion channels types.

So far, structural studies have resulted in a discrete number of "frozen" conformations, which could only be set in motion by MD with a time limit of the order of μs. However, these limitations could also be overcome. With the development of XFEL, the time-resolved serial crystallography method has allowed dynamic patterns of ion channel activation to be obtained [134].

## FUNDING

This work was supported by RFBR grant nos. 18-504-12045 (ion channels in SMA) and 20-54-15004 (structure and physiology of KCNH2 and KCNQ1 channels). G.L. has been supported by the CNRS grant PRC RUSSIE 2019 (PRC no. 2773).

## REFERENCES

1. S. K. Natchiar, A. G. Myasnikov, H. Kratzat, et al., Nature **551** (7681), 472 (2017). https://doi.org/10.1038/nature24482
2. Y. Suo, Z. Wang, L. Zubcevic, et al., Neuron. **105** (5), 882 (2020). https://doi.org/10.1016/j.neuron.2019.11.023
3. W. Wang and R. MacKinnon, Cell **169** (3), 422 (2017). https://doi.org/10.1016/j.cell.2017.03.048
4. S. Chakraborty, M. Jasnin, and W. Baumeister, Protein Sci. **29** (6), 1302 (2020). https://doi.org/10.1002/pro.3858
5. A. P. Owji, Z. Qingqing, J. Changyi, et al., Nat. Struct. Mol. Biol. **27** (4), 382 (2020). https://doi.org/10.1038/s41594-020-0402-z
6. S. Schmid and T. Hugel, Elife **9** (2020). https://doi.org/10.7554/eLife.57180
7. T. Jespersen, M. Grunnet, and S. P. Olesen, Physiology (Bethesda) **20**, 408 (2005). https://doi.org/10.1152/physiol.00031.2005
8. D. Peroz, N. Rodriguez, F. Choveau, et al., J. Physiol. **586** (7), 1785 (2008). https://doi.org/10.1113/jphysiol.2007.148254
9. P. Duggal, M. R. Vesely, D. Wattanasirichaigoon, et al., Circulation **97** (2), 42 (1998). https://doi.org/10.1161/01.cir.97.2.142
10. Y. H. Chen, S.-J. Xu, S. Bendahhou, et al., Science **299** (5604), 251 (2003). https://doi.org/10.1126/science.1077771
11. J. L. Smith, C. L. Anderson, D. E. Burgess, et al., J. Arrhythm. **32** (5), 373 (2016). https://doi.org/10.1016/j.joa.2015.11.009
12. M. Koponen, A. S. Havulinna, A. Marjamaa, et al., BMC Med. Genet. **19** (1), 56 (2018). https://doi.org/10.1186/s12881-018-0574-0
13. D. J. Tester and M. J. Ackerman, Methodist Debakey Cardiovasc. J. **10** (1), 29 (2014). https://doi.org/10.14797/mdcj-10-1-29
14. D. Hu, L. Yang, Z. Jiancheng, et al., JACC Clin. Electrophysiol. **3** (7), 727 (2017). https://doi.org/10.1016/j.jacep.2016.11.013
15. Q. I. Wang, O. Seiko, W.-G. Ding, et al., J. Cardiovasc. Electrophysiol. **25** (5), 522 (2014). https://doi.org/10.1111/jce.12361
16. K. Hong, P. Bjerregaard, I. Gussak, et al., J. Cardiovasc. Electrophysiol. **16** (4), 394 (2005). https://doi.org/10.1046/j.1540-8167.2005.40621.x
17. H. Hishigaki and S. Kuhara, Database (Oxford) bar017 (2011). https://doi.org/10.1093/database/bar017
18. M. C. Sanguinetti, J. Chen, D. Fernandez, et al., Novartis Found Symp. **266**, 159 (2005).
19. S. P. Etheridge, S. Y. Asaki, and M. C. Niu, Curr. Opin. Cardiol. **34** (1), 46 (2019). https://doi.org/10.1097/HCO.0000000000000587
20. M. Li, Y. N. Jan, and L. Y. Jan, Science **257** (5074), 1225 (1992). https://doi.org/10.1126/science.1519059
21. D. A. Doyle, J. M. Cabral, R. A. Pfuetzner, et al., Science **280** (5360), 69 (1998). https://doi.org/10.1126/science.280.5360.69
22. A. Kreusch, P. J. Pfaffinger, C. F. Stevens, et al., Nature **392** (6679), 945 (1998). https://doi.org/10.1038/31978
23. W. R. Kobertz, C. Williams, and C. Miller, Biochemistry **39** (34), 10347 (2000). https://doi.org/10.1021/bi001292j
24. O. Sokolova, L. Kolmakova-Partensky, and N. Grigorieff, Structure **9** (3), 215 (2001). https://doi.org/10.1016/s0969-2126(01)00578-0
25. S. B. Long, E. B. Campbell, and R. Mackinnon, Science **309** (5736), 897 (2005). https://doi.org/10.1126/science.1116269
26. A. V. Grizel, G. S. Glukhov, and O. S. Sokolova, Acta Nat. **6** (4), 10 (2014).
27. K. S. Glauner, L. M. Mannuzzu, C. S. Gandhi, and E. Y. Isacoff, Nature **402** (6763), 813 (1999). https://doi.org/10.1038/45561

28. T. Ferrer, J. Rupp, D. R. Piper, and M. Tristani-Firouzi, J. Biol. Chem. **281** (18), 12858 (2006). https://doi.org/10.1074/jbc.M513518200
29. S. Y. Lee, A. Lee, J. Chen, et al., Proc. Natl. Acad. Sci. U. S. A. **102** (43), 15441 (2005). https://doi.org/10.1073/pnas.0507651102
30. G. Yellen, Nature **419** (6902), 35 (2002). https://doi.org/10.1038/nature00978
31. J. Holyoake, C. Domene, J. Bright, et al., Eur. Biophys. J. **33** (3), 238 (2004). https://doi.org/10.1007/s00249-003-0355-2
32. M. Jensen, V. Jogini, D. Borhani, et al., Science **336** (6078), 229 (2012). https://doi.org/10.1126/science.1216533
33. G. E. Flynn and W. N. Zagotta, Neuron **30** (3), 689 (2001). https://doi.org/10.1016/s0896-6273(01)00324-5
34. R. MacKinnon and G. Yellen, Science **250** (4978), 276 (1990). https://doi.org/10.1126/science.2218530
35. A. J. Yool and T. L. Schwarz, Nature **349** (6311), 700 (1991). https://doi.org/10.1038/349700a0
36. Y. Liu, M. Holmgren, M. Jurman, et al., Neuron **19** (1), 175 (1997). https://doi.org/10.1016/s0896-6273(00)80357-8
37. B. C. Schroede, S. Waldegger, S. Fehr, et al., Nature **403** (6766), 196 (2000). https://doi.org/10.1038/35003200
38. J. Barhanin, F. Lesage, E. Guillemare, et al., Nature **384** (6604), 78 (1996). https://doi.org/10.1038/384078a0
39. M. C. Sanguinetti, M. Curran, A. Zou, et al., Nature **384** (6604), 80 (1996). https://doi.org/10.1038/384080a0
40. G. Loussouarn, I. Baró, and D. Escand, Methods Mol. Biol. **337**, 167 (2006). https://doi.org/10.1385/1-59745-095-2:167
41. M. Keating, Circulation **85** (6), 1973 (1992). https://doi.org/10.1161/01.cir.85.6.1973
42. D. J. Tester, M. Will, C. Haglund, et al., Heart Rhythm **2** (5), 507 (2005). https://doi.org/10.1016/j.hrthm.2005.01.020
43. J. B. Gourraud, J. Barc, A. Thollet, et al., Front. Cardiovasc. Med. **3**, 9 (2016). https://doi.org/10.3389/fcvm.2016.00009
44. V. Probst, A. Wilde, J. Barc, et al., Circ. Cardiovasc. Genet. **2** (6), 552 (2009). https://doi.org/10.1161/CIRCGENETICS.109.853374
45. G. Loussouarn, K.-H. Park, C. Bellocq, et al., EMBO J. **22** (20), 5412 (2003). https://doi.org/10.1093/emboj/cdg526
46. N. Rodriguez, M. Amarouch, J. Montnach, et al., Biophys. J. **99** (4), 1110 (2010). https://doi.org/10.1016/j.bpj.2010.06.013
47. K. H. Park, J. Piron, S. Dahimene, et al., Circ. Res. **96** (7), 730 (2005). https://doi.org/10.1161/01.RES.0000161451.04649.a8
48. F. S. Choveau, N. Rodriguez, F. Abderemane, et al., J. Biol. Chem. **286** (1), 707 (2011). https://doi.org/10.1074/jbc.M110.146324
49. O. A. Malak, Z. Es-Salah-Lamoureux, and G. Loussouarn, Sci. Rep. **7** (1), 113 (2017). https://doi.org/10.1038/s41598-017-00155-2
50. O. A. Malak, G. Gluhov, A. Grizel, et al., J. Biol. Chem. **294** (16), 6506 (2019). https://doi.org/10.1074/jbc.RA119.007626
51. O. A. Malak, F. Abderemane-Ali, Y. Wei, et al., Sci. Rep. **10** (1), 5852 (2020). https://doi.org/10.1038/s41598-020-62615-6
52. C. A. Ng, M. D. Perry, W. Liang, et al., Heart Rhythm **17** (3), 492 (2020). https://doi.org/10.1016/j.hrthm.2019.09.020
53. C. G. Vanoye, R. Desai, K. Fabreet, et al. Circ. Genom. Precis. Med. **11** (11), e002345 (2018). https://doi.org/10.1161/CIRCGEN.118.002345
54. T. Takumi, H. Ohkubo, and S. Nakanishi, Science **242** (4881), 1042 (1988). https://doi.org/10.1126/science.3194754
55. I. Ben-Efraim, D. Bach, and Y. Shai, Biochemistry **32** (9), 2371 (1993). https://doi.org/10.1021/bi00060a031
56. F. Lesage, B. Attali, J. Lakey, et al., Receptors Channels **1** (2), 143 (1993).
57. R. van Huizen, D. Czajkowsky, D. Shi, et al., FEBS Lett. **457** (1), 107 (1999). https://doi.org/10.1016/s0014-5793(99)01021-2
58. M. Li, M. Li, N. Unwin, et al., Curr. Biol. **4** (2), 110 (1994). https://doi.org/10.1016/s0960-9822(94)00026-6
59. E. V. Orlova, M. Papakosta, F. Booy, et al., J. Mol. Biol. **326** (4), 1005 (2003). https://doi.org/10.1016/s0022-2836(02)00708-8
60. O. Sokolova, A. Accardi, D. Gutierrez, et al., Proc. Natl. Acad. Sci. U. S. A. **100** (22), 12607 (2003). https://doi.org/10.1073/pnas.2235650100
61. M. Wolf, A. Eberhart, H. Glossmann, et al., J. Mol. Biol. **332** (1), 171 (2003). https://doi.org/10.1016/s0022-2836(03)00899-4
62. Q. X. Jiang, D. N. Wang, and R. MacKinnon, Nature **430** (7001), 806 (2004). https://doi.org/10.1038/nature02735
63. M. Samsó, T. Wagenknecht, and P. D. Allen, Nat. Struct. Mol. Biol. **12** (6), 539 (2005). https://doi.org/10.1038/nsmb938
64. I. I. Serysheva, S. Ludtke, M. Baker, et al., Proc. Natl. Acad. Sci. U. S. A. **105** (28), 9610 (2008). https://doi.org/10.1073/pnas.0803189105
65. M. Mishyna, O. Volokh, Y. Danilova, et al., Micron **96**, 57 (2017). https://doi.org/10.1016/j.micron.2017.02.004
66. A. F. Brilot, J. Chen, A. Cheng, et al., J. Struct. Biol. **177** (3), 630 (2012). https://doi.org/10.1016/j.jsb.2012.02.003
67. P. J. Corringer, M. Baaden, N. Bocquetet, et al., J. Physiol. **588** (4), 565 (2010). https://doi.org/10.1113/jphysiol.2009.183160
68. A. Kuo, J. Gulbis, J. Antcliff, et al., Science **300** (5627), 1922 (2003). https://doi.org/10.1126/science.1085028

69. Y. Jiang, A. Lee, J. Chenet, et al., Nature **423** (6935), 33 (2003). https://doi.org/10.1038/nature01580
70. T. Kawate, J. Michel, W. Birdsong, and E. Gouaux, Nature **460** (7255), 592 (2009). https://doi.org/10.1038/nature08198
71. S. B. Long, X. Tao, E. Campbell, and R. MacKinnon, Nature **450** (7168), 376 (2007). https://doi.org/10.1038/nature06265
72. S. G. Brohawn, J. del Mármol, and R. MacKinnon, Science **335** (6067), 436 (2012). https://doi.org/10.1126/science.1213808
73. M. Liao, E. Cao, D. Julius, et al., Nature **504** (7478), 107 (2013). https://doi.org/10.1038/nature12822
74. S. H. Scheres, Methods Enzymol. **579**, 125 (2016). https://doi.org/10.1016/bs.mie.2016.04.012
75. J. R. Whicher and R. MacKinnon, Science **353** (6300), 664 (2016). https://doi.org/10.1126/science.aaf8070
76. J. Sun and R. MacKinnon, Cell **169** (6), 1042 (2017). https://doi.org/10.1016/j.cell.2017.05.019
77. Y. Jiang, V. Ruta, J. Chen, et al., Nature **423** (6935), 42 (2003). https://doi.org/10.1038/nature01581
78. É. Lörinczi, J. Camilo Gómez-Posada, P. de la Peña, et al., Nat. Commun. **6**, 6672 (2015). https://doi.org/10.1038/ncomms7672
79. T. Ferrer, J. Rupp, D. Piper, et al., J. Biol. Chem. **281** (18), 12858 (2006). https://doi.org/10.1074/jbc.M513518200
80. G. F. Schertler, C. Villa, and R. Henderson, Nature **362** (6422), 770 (1993). https://doi.org/10.1038/362770a0
81. N. Unwin, Nature **373** (6509), 37 (1995). https://doi.org/10.1038/373037a0
82. Q. X. Jiang, D. W. Chester, and F. J. Sigworth, J. Struct. Biol. **133** (2–3), 119 (2001). https://doi.org/10.1006/jsbi.2001.4376
83. Y. N. Antonenko, G. Gluhov, A. Firsov, et al., Phys. Chem. Chem. Phys. **17** (26), 17461 (2015). https://doi.org/10.1039/c5cp02047f
84. P. S. Marius, J. East Alvis, and A. Lee, Biophys. J. **89** (6), 4081 (2005). https://doi.org/10.1529/biophysj.105.070755
85. X. Liu, G. Wu, Y. Yu, et al., PLoS Biol. **17** (4), e3000096 (2019). https://doi.org/10.1371/journal.pbio.3000096
86. N. Yoder and E. Gouaux, Elife **9** (2020). https://doi.org/10.7554/eLife.56527
87. C. A. Peters-Libeu, Y. Newhouse, S. Hall, et al., J. Lipid. Res. **48** (5), 1035 (2007). https://doi.org/10.1194/jlr.M600545-JLR200
88. N. T. Johansen, F. Tidemand, T. Nguyen Tam, et al., FEBS J. **286** (9), 1734 (2019). https://doi.org/10.1111/febs.14766
89. Z. Zhao, M. Zhang, J. Hogle, et al., J. Am. Chem. Soc. **140** (34), 10639 (2018). https://doi.org/10.1021/jacs.8b04638
90. M. L. Nasr, D. Baptista, M. Strauss, et al., Nat. Methods **14** (1), 49 (2017). https://doi.org/10.1038/nmeth.4079
91. F. Hagn, M. L. Nasr, and G. Wagner, Nat. Protoc. **13** (1), 79 (2018). https://doi.org/10.1038/nprot.2017.094
92. M. S. Reid, D. M. Kern, and S. G. Brohawn, Elife **9** (2020). https://doi.org/10.7554/eLife.52505
93. B. Gardill, J. Huang, L. Tu, et al., Sci. Rep. **10** (1), 1130 (2020). https://doi.org/10.1038/s41598-020-58002-w
94. J. Sun and R. MacKinnon, Cell **180** (2), 340 (2020). https://doi.org/10.1016/j.cell.2019.12.003
95. L. Zhou and L. A. Sazanov, Science **365** (6455) (2019). https://doi.org/10.1126/science.aaw9144
96. S. Feng, S. Dang, T. Han, et al., Cell. Rep. **28** (2), 567e4 (2019). https://doi.org/10.1016/j.celrep.2019.06.023
97. C. C. Su, C. Morgan, S. Kambakam, et al., mBio **10**, 4 (2019). https://doi.org/10.1128/mBio.01295-19
98. D. M. Kern, S. Oh, R. Hite, et al., Elife **8** (2019). https://doi.org/10.7554/eLife.42636
99. S. Sharma, R. Oot, M. Khan, and S. Wilkens, J. Biol. Chem. **294** (16), 6439 (2019). https://doi.org/10.1074/jbc.RA119.007577
100. H. E. Autzen, A. Myasnikov, M. Campbell, et al., Science **359** (6372), 228 (2018). https://doi.org/10.1126/science.aar4510
101. A. F. Kintzer, E. Green, P. Dominik, et al., Proc. Natl. Acad. Sci. U. S. A. **115** (39), E9095 (2018). https://doi.org/10.1073/pnas.1805651115
102. D. Matthies, O. Dalmas, M. Borgnia, et al., Cell **164** (4), 747 (2016). https://doi.org/10.1016/j.cell.2015.12.055
103. Z. O. Shenkarev, M. Karlova, D. Kulbatskii, et al., Biochemistry **83** (5), 562 (2018). https://doi.org/10.1134/S0006297918050097
104. C. Gatsogiannis, F. Merino, D. Prumbaum, et al., Nat. Struct. Mol. Biol. **23** (10), 884 (2016). https://doi.org/10.1038/nsmb.3281
105. Y. Gao, E. Cao, D. Julius, and Y. Cheng, Nature **534** (7607), 347 (2016). https://doi.org/10.1038/nature17964
106. S. R. Tonge and B. J. Tighe, Adv. Drug. Deliv. Rev. **53** (1), 109 (2001). https://doi.org/10.1016/s0169-409x(01)00223-x
107. S. Scheidelaar, M. Koorengevel, C. van Walree, et al., Biophys. J. **111** (9), 1974 (2016). https://doi.org/10.1016/j.bpj.2016.09.025
108. A. Colbasevici, N. Voskoboynikova, P. Orekhov, et al., Biochim. Biophys. Acta, Biomembr. **1862** (5), 183207 (2020). https://doi.org/10.1016/j.bbamem.2020.183207
109. J. J. Domínguez Pardo, M. Koorengevel, N. Uwugiaren, et al., Biophys. J. **115** (1), 129 (2018). https://doi.org/10.1016/j.bpj.2018.05.032
110. R. Zhang, I. Sahu, L. Liu, et al., Biochim. Biophys. Acta **1848** (1), Pt. B, **329** (2015). https://doi.org/10.1016/j.bbamem.2014.05.008

111. S. Scheidelaar, M. Koorengevel, J. Dominguez Pardo, et al., Biophys. J. **108** (2), 279 (2015). https://doi.org/10.1016/j.bpj.2014.11.3464

112. J. J. Dominguez Pardo, J. Dörr, A. Iyer, et al., Eur. Biophys. J. **46** (1), 91 (2017). https://doi.org/10.1007/s00249-016-1181-7

113. R. Cuevas Arenas, J. Klingler, C. Vargas, and S. Keller, Nanoscale **8** (32), 15016 (2016). https://doi.org/10.1039/c6nr02089e

114. J. M. Dörr, M. van Coevorden-Hameete, C. Hoogenraad, and J. Killian, Biochim. Biophys. Acta Biomembr. **1859** (11), 2155 (2017). https://doi.org/10.1016/j.bbamem.2017.08.010

115. T. J. Knowles, R. Finka, C. Smith, et al., J. Am. Chem. Soc. **131** (22), 7484 (2009). https://doi.org/10.1021/ja810046q

116. S. Gulati, M. Jamshad, T. Knowles, et al., Biochem. J. **461** (2), 269 (2014). https://doi.org/10.1042/BJ20131477

117. A. R. Long, C. O'Brien, K. Malhotra, et al., BMC Biotechnol. **13**, 41 (2013). https://doi.org/10.1186/1472-6750-13-41

118. M. G. Karlova, N. Voskoboynikova, G. Gluhov, et al., Chem. Phys. Lipids **219**, 50 (2019). https://doi.org/10.1016/j.chemphyslip.2019.01.013

119. M. Jamshad, J. Charlton, Y. Lin, et al., Biosci. Rep. **35** (2) (2015). https://doi.org/10.1042/BSR20140171

120. J. M. Dörr, M. Koorengevel, M. Schäfer, et al., Proc. Natl. Acad. Sci. U. S. A. **111** (52), 18607 (2014). https://doi.org/10.1073/pnas.1416205112

121. V. Postis, S. Rawson, J. Mitchell, et al., Biochim. Biophys. Acta **1848** (2), 496 (2015). https://doi.org/10.1016/j.bbamem.2014.10.018

122. D. J. Swainsbury, S. Scheidelaar, R. van Grondelle, et al., Angew. Chem. Int. Ed. Engl. **53** (44), 11803 (2014). https://doi.org/10.1002/anie.201406412

123. V. Schmidt, M. Sidore, C. Bechara, et al., Biochim. Biophys. Acta Biomembr. **1861** (2), 431 (2019). https://doi.org/10.1016/j.bbamem.2018.10.017

124. D. J. K. Swainsbury, M. Proctor, A. Hitchcock, et al., Biochim. Biophys. Acta Bioenerg. **1859** (3), 215 (2018). https://doi.org/10.1016/j.bbabio.2017.12.005

125. I. Prabudiansyah, I. Kusters, A. Caforio, and A. Driessen, Biochim. Biophys. Acta **1848** (10), part A, 2050 (2015). https://doi.org/10.1016/j.bbamem.2015.06.024

126. J. S. van't Klooster, T. Cheng, H. Sikkema, et al., Elife **9** (2020). https://doi.org/10.7554/eLife.57003

127. M. Parmar, S. Rawson, C. Scarff, et al., Biochim. Biophys. Acta Biomembr. **1860** (2), 378 (2018). https://doi.org/10.1016/j.bbamem.2017.10.005

128. M. Hernando, G. Orriss, J. Perodeau, et al., Biochim. Biophys. Acta Biomembr. **1862** (5), 183191 (2020). https://doi.org/10.1016/j.bbamem.2020.183191

129. R. M. Johnson, C. Fais, M. Parmar, et al., Microorganisms **8** (6), 943 (2020). https://doi.org/10.3390/microorganisms8060943

130. C. Sun, S. Benlekbir, P. Venkatakrishnan, et al., Nature **557** (7703), 123 (2018). https://doi.org/10.1038/s41586-018-0061-y

131. J. Standfuss, Curr. Opin. Struct. Biol. **57**, 63 (2019). https://doi.org/10.1016/j.sbi.2019.02.001

132. M. Caffrey and V. Cherezov, Nat. Protoc. **4** (5), 706 (2009). https://doi.org/10.1038/nprot.2009.31

133. V. Cherezov, D. Rosenbaum, M. Hanson, et al., Science **318** (5854), 1258 (2007). https://doi.org/10.1126/science.1150577

134. P. Nogly, T. Weinert, D. James, et al., Science **361** (6398), eaat0094 (2018). https://doi.org/10.1126/science.aat0094

135. E. C. Twomey and A. I. Sobolevsky, Biochemistry **57** (3), 267 (2018). https://doi.org/10.1021/acs.biochem.7b00891